THE ASTROPHYSICAL JOURNAL, 322:88–100, 1987 November 1

ARECIBO OBSERVATIONS OF *IRAS* GALAXIES AT 21 AND 18 CENTIMETERS

ROBERT W. GARWOOD
Department of Astronomy, University of Minnesota
GEORGE HELOU
Infrared Processing and Analysis Center, California Institute of Technology
AND
JOHN M. DICKEY
Department of Astronomy, University of Minnesota
Received 1986 July 28; accepted 1987 April 23

ABSTRACT

We report Arecibo observations at 21 cm and 18 cm of a sample of galaxies selected for their intense far-infrared (FIR) emission. The objective was to search for H I absorption and OH maser emission. No new cases were found. We discuss the significance of this null result both in terms of the spatial distribution of the interstellar gas and dust and in terms of the continuum luminosity of the nucleus. Nevertheless, the H I profiles are extraordinary in that most are convex (single peak). This may suggest disruption of the disk rotation system in some cases.

We find little correlation between the hydrogen mass of these galaxies and their FIR luminosity. Comparison of these quantities suggests that the dust in these galaxies is under conditions very different from the solar neighborhood. Much more of the FIR emission apparently comes from H II regions than in normal galaxies. There is an excellent correlation between IR flux and radio continuum flux. The ratio of these two is the same as for normal spirals, which is surprising considering the many variables which could change this ratio.

Subject headings: galaxies: photometry — infrared: sources — radio sources: galaxies — radio sources: 21 cm radiation

I. INTRODUCTION

The discovery by *IRAS* of strong far-infrared (FIR) emission from many galaxies forces a reevaluation of the energy balance in these systems, especially when a substantial fraction of the luminosity is emitted in the infrared (Soifer *et al.* 1984*b*, 1986). Many of the luminous *IRAS* galaxies are powered by star formation alone, so it is in the interstellar medium itself that one should look for the origin of the remarkable luminosities involved. Hence the interest in studying the interstellar medium in these infrared-bright objects. The search for mechanisms that may lead to episodes of accelerated star formation will not only help explain the very luminous sources, and possibly provide a genetic link between starbursts and quasars (Beichman *et al.* 1986; Wilson 1987; Rodriguez Espinosa, Rudy, and Jones 1987), but will also help illuminate the star-formation process in the more quiescent "normal" spiral galaxies.

In order to address the questions above, one has first to obtain the various data relevant to the phenomena, develop a correct interpretation of each of the measurements (e.g., what fraction of the infrared flux is directly associated with star formation?), and then proceed to the analysis. Crucial galaxy parameters in this connection include infrared emission, emission in the atomic and molecular lines (Young *et al.* 1986; Sanders and Mirabel 1985), Hα and radio continuum emission (Kennicutt 1983*a*, *b*).

As a first effort in this direction, we have surveyed at the 21 cm H I line and at the 18 cm OH lines a sample of infrared-selected galaxies compiled from the *IRAS* minisurvey (Soifer *et al.* 1984*a*) and from the *IRAS Point Source Catalog* (PSC) (1985). Sample selection is discussed in § II below, together with the observations, carried out at Arecibo. Section III gives the H I and OH data (line integrals or upper limits, line widths, improved redshifts), measurements for the continuum emission at 21 cm, and the *IRAS* data, as well as comments on individual objects. Section IV discusses the implications of the data, addressing in particular the properties of the sample galaxies as compared to "normal" disk galaxies, the correlation between radio and infrared, and the relation between infrared on one hand and H I and OH line emission on the other.

II. SAMPLE AND OBSERVATIONS

The selection of galaxies for this survey was primarily based on *IRAS Circular* No. 6 (1983), which is the infrared-complete sample of galaxies found in the *IRAS* minisurvey and analyzed by Soifer *et al.* (1984*a*). Selection for observation involved two requirements: first, that a source be within the Arecibo declination range; and second, that it have a known redshift within reach of the available Arecibo feed-receiver combinations. Of the 86 *IRAS* minisurvey sources associated with galaxies, 67 are within the Arecibo declination range (0 to 36 deg), but only half of these could be found in optical catalogs. Redshifts were therefore taken mostly from a spectroscopic survey by C. Lonsdale *et al.* (private communication). In the end, 17 sources from *IRAS Circular* No. 6 were chosen for observation.

The remaining 18 sources observed were selected from *Cataloged Galaxies and Quasars Observed in the IRAS Survey* (1985, hereafter CGQ) with the same two requirements as above, and the condition that their 60 μm flux density as listed in CGQ be greater than 5 Jy. Of the 35 galaxies on the final observing list, 30 were observed at 21 cm, 31 were observed at 18 cm, and 21 cm continuum measurements were made on 27 sources.

The observations were made during 1985 January and February using the 305 m reflector of the Arecibo Observatory. For H I line observations at redshifts smaller than 4500 km s^{-1}, the 40 foot (12 m) dual circular feed was used, tuned to 1415 MHz. Higher redshift observations were made with the new 22 cm, continuously tunable feed, using only two settings corresponding respectively to 1395 and 1375 MHz. The OH line observations were made using the 18 cm dual circular feed. The feeds used were quite similar in their beams (full beam width at half-power about 3′), and their peak sensitivity (about 8 K Jy^{-1}). The receivers for all of the observations are similar, with system temperatures about 40 to 50 K.

The total power observing mode was used throughout the observations with 5 minutes on-source and 5 minutes on blank sky, about 6 minutes of right ascension east of the on-source position. The continuum measurements were made using drift scans across the source and 1′ north and south of the source. System gain calibration was tied to the flux densities given in Bridle *et al.* (1972) for the following reference sources: 3C 48, 1710+16, 1843+09, 3C 133, and 3C 298. These same sources were observed in the spectral line mode as bandpass calibrators as well as during the continuum observations. For all spectral line observations, the 1008 channel autocorrelator was divided into four quadrants of 252 channels each (two quadrants for each polarization). A total bandwidth of about 10 MHz was observed, resulting in a channel spacing of 8.3 km s^{-1} at 21 cm and 7 km s^{-1} at 18 cm. The spectral resolution after Hanning smoothing is about twice the channel separation. The four autocorrelator quadrants were averaged together, a zenith angle correction was applied, and the frequency dependence of the system was removed. Baselines were fitted to and then subtracted from the unsmoothed spectra.

III. DATA

The observational, measured, and calculated quantities are summarized in Table 1. Each source listing consists of two lines. Two galaxies dominated by H I absorption (U9913 = Arp 220 and U10592 = NGC 6240) are listed at the end of Table 1. Following is a description of the entries in each column.

Column (1) gives a source name, usually the primary identification (col. [2] of right-hand page) in CGQ. For five sources that do not appear in CGQ, the *IRAS* PSC names are given. Source name is followed in column (2) by a number indicating whether this source was chosen from *IRAS Circular* No. 6 (numeral 1) or from CGQ (numeral 2) as described above. Column (3) gives the NGC or IC identification, again taken from CGQ.

Column (4) lists the right ascension and declination (1950 equinox) which were actually observed. These correspond usually to the position of the *IRAS* point source. UGC 9903 and 10024, both galaxies with known companions, were observed at multiple positions which are indicated as multiple entries in Table 1. Source names U9903C and U10024C correspond to the *IRAS* positions, U10024N to the position for the companion of U10024 (Z1543.7+0236), and U9903A to the position of U9904.

Column (5) lists the optical major and minor axis sizes in arcminutes. These are generally from the Uppsala General Catalog (Nilson 1973) with the exception of two galaxies (Z0357.8+2055, Z0415.1+0.125) which come from the *Morphological Catalog of Galaxies* (Vorontsov-Velyaminov and Arhipova 1963–1974; Vorontsov-Velyaminov and Krasnogorskaja 1962).

Column (6) (B_T) gives the total blue magnitude on the system defined by the *Second Reference Catalogue of Bright Galaxies* (de Vaucouleurs, de Vaucouleurs, and Corwin 1976) (hereafter RC2). If the magnitude is followed by an R, then it is actually taken from RC2. If it is followed by a Z, then it is taken from a Zwicky magnitude adjusted to the B_T scale by a statistical correction following the prescription in Kirshner *et al.* (1978). The second line in column (6) lists B_T^G, the blue magnitude corrected for Galactic extinction. The correction adopted is the average of the corrections recommended in RC2 and the revised Shapley-Ames Catalog (Sandage and Tammann 1981). No correction has been made to B_T for self-absorption in the galaxy itself. Such a correction is a function of inclination and type, both of which are parameters poorly determined in this sample which contains many optically peculiar objects.

Columns (7) (S_{60}) and (8) (S_{100}) list the 60 and 100 μm flux density (Jy) from the *IRAS* PSC. In the few cases where only an upper limit was available in the PSC, the 60 and 100 μm values were obtained from the *IRAS* raw data by co-addition of all the data from all the individual detectors that scanned the position of the galaxy. Column (9) gives log (FIR), defined in CGQ, and proposed as a good estimate of the flux from a galaxy between 42.5 and 122.5 μm:

$$\mathrm{FIR} = 1.26 \times 10^{-14} \times [2.58 f_\nu(60\ \mu\mathrm{m}) + f_\nu(100\ \mu\mathrm{m})]\ \mathrm{W\ m^{-2}},$$

where f_ν are the flux densities in Jy measured by *IRAS*.

Column (10) lists the rms of the noise (mJy) after baseline removal for the 21 cm observations (σ_{21}, line [1] of each source) and for the 18 cm observations (σ_{18}, line [2]). A blank in either line means that no observations were made at that wavelength for that source. For galaxies detected at 21 cm, column [11] gives the peak signal-to-noise ratio in the spectrum. The feed used for the 21 cm observations is indicated by a number in column (12) (a "1" for the 40 foot dual circular feed and a "2" for the 22 cm tunable feed).

Line (1) under column (13) lists the measured heliocentric velocity in km s^{-1} (V_h). Line (2) gives the systemic velocity corrected to the Local Group of galaxies (V_0) using the results of Yahil, Tammann, and Sandage (1977). For galaxies not detected, velocities, in parentheses, from Lonsdale *et al.* (private communication) are shown. Column (14) (W_{50}) lists the 50% width of the profile. Heliocentric redshift and profile width are the midpoint and the difference between the points at which the line emission falls to half the (closer) peak value in the emission profile. Column (15) (FI) shows the profile integral in Jy km s^{-1}. The flux integral for three galaxies not observed (U1201, U10182, U10439) and one galaxy not detected at 21 cm are taken from the literature. The sources for these values are indicated in the footnotes to the table and in the notes on individual galaxies. As can be seen in column (5) a few galaxies are comparable in angular size with the 3′.1 beam of the telescope. Consequently, the profile integral will be seriously underestimated for these galaxies. A correction factor is calculated assuming an angular size in H I equal to 1.2 times the major axis and assuming a Gaussian beam of 3′.1 FWHM. Correction factors calculated in this manner are typically within 10% of the correction factors calculated in Haynes and Giovanelli (1984). The corrected flux integral (FI_C) is shown on line (2) of column (15). Those galaxies without sizes listed in column (5) are small and the correction factors are negligible.

TABLE 1

MEASURED AND CALCULATED QUANTITIES FOR OBSERVED GALAXIES

Galaxy (1)	C (2)	NGC/IC (3)	R.A. Decl. (4)	$a \times b$ (5)	B_T B_T^G (6)	S_{60} (Jy) (7)	S_{100} (Jy) (8)	log FIR (W m^{-2}) (9)
U966	2	N520	12159.6 +33152	5.0 × 2.0	12.05R 11.94	31.21	47.41	−11.79
U1201	2	N660	14021.6 +132341	10.0 × 4.5	11.5R 11.3	64.99	102.38	−11.47
III Zw 035	2		14148.1 +165107	...	... ...	13.11	13.40	−12.23
U1304	2	N693	14754.2 +55352	3.2 × 1.6	13.2Z 13.2	8.50	11.80	−12.37
U1315	2	N695	14828.0 +222008	0.5 × 0.5	13.5Z 13.3	8.00	13.06	−12.37
U1351	2	I1743	15018.3 +122744	2.1 × 0.9	13.8Z 13.7	6.19	12.12	−12.45
U1451	2		15541.4 +250703	1.3 × 0.7	14.1Z 13.9	6.65	12.66	−12.43
U1720	2	I214	21128.4 +45629	0.9 × 0.6	14.2Z 14.1	5.28	8.18	−12.56
U1768	2	N877	21515.2 +141837	2.3 × 1.8	12.50R 12.33	13.75	29.00	−12.09
U2103	2	N992	23435.8 +205306	0.9 × 0.7	13.3Z 13.1	10.04	16.44	−12.27
U2365	2	N1134	25057.1 +124842	2.5 × 0.9	13.0Z 12.8	8.97	17.24	−12.29
Z0355.3+1826	1	N1488	35518.3 +182631	...	15.3Z 15.0	0.60	1.70	−13.39
Z0356.6+2140	1		35632.2 +213916	...	15.1Z 14.7	0.71	1.70	−13.35
Z0357.8 + 2055	1		35743.0 +205432	0.5 × 0.5	15.3Z 15.0	0.54	1.34	−13.46
U2970	1	N1517	40629.0 +83103	1.2 × 1.1	14.1Z 13.8	3.37	6.88	−12.71
U2982	1		40943.7 +52512	1.0 × 0.5	15.3Z 15.1	8.32	15.70	−12.33
IRAS 04120+0622	1		41204.8 +62210	...	... ...	0.64	1.20	−13.44
U2997	1		41323.0 +80322	1.2 × 0.6	14.8Z 14.5	4.58	5.33	−12.67
IRAS 04139+0238 (U2998)	1		41358.7 +23809	1.6 × 1.5	14.7Z 14.5	0.64	3.00	−13.23
IRAS 04144+1020	1		41428.6 +102002	...	... ...	2.53	7.40	−12.76
IRAS 04147+0218 (U3004)	1		41442.9 +21845	1.5 × 1.0	14.7Z 14.5	1.50	4.00	−13.00
Z0415.1+0125	1		41507.3 +12621	0.5 × 0.4	14.7Z 14.5	2.79	5.80	−12.79
U3014	1		41716.5 +15825	1.4 × 0.8	14.5Z 14.3	0.88	1.93	−13.28
U9903A (U9904)	2	N5954	153215.7 +152213	1.1 × 0.5	13.5Z 13.3	...	...	...
U9903B			153209.7 +152100	...	...	...	...	...
U9903C		N5953	153213.3 +152142	1.7 × 1.3	13.1Z 12.9	10.24	19.71	−12.24
U9903D			153220.5 +152046	...	... ...	...	...	...
U9903E			153210.6 +152340	...	... ...	...	...	...
U9926	2	N5962	153413.8 +164616	2.8 × 2.0	12.05R 11.90	8.46	21.35	−12.26
U10024C	2	N5990	154344.7 +23411	1.6 × 0.9	12.9Z 12.7	9.76	15.35	−12.29
U10024N (Z1543.7+0236)			154341.8 +23622	...	... ...	...	...	...
U10182	2	N6052	160302.6 +204035	0.8 × 0.6	13.45R 13.27	6.94	9.74	−12.46
U10439	2	N6181	163010.1 +195549	2.5 × 1.0	12.50R 12.28	8.75	19.85	−12.37
16547+0257	1		165442.4 +25734	...	... ...	1.85	2.08	−13.06
Z1658.7+0656	1		165842.9 +65547	...	15.2Z 14.9	1.32	2.05	−13.16
Z1710.1+1637	1		171009.2 +163712	...	15.3Z 15.1	0.48	2.00	−13.39
U11035	1		175239.1 +325336	1.7 × 1.1	14.1Z 13.8	3.42	6.81	−12.71
U11041	1		175304.5 +344659	1.3 × 0.8	13.7Z 13.4	5.84	13.03	−12.45
U9913 (ARP 220)	2	I4553	153246.3 +234010	2.0 × 1.8	14.2Z 14.1	103.68	116.25	−11.32
U10592	2	N6240	165027.7 +22858	2.2 × 0.9	14.5Z 14.1	23.32	25.88	−11.97

[a] Giovanardi and Krumm 1983.
[b] Gordon and Gottesman 1981.
[c] Beiging and Biermann 1983.
[d] Krumm and Salpeter 1980.

TABLE 1—*Continued*

σ_{21} / σ_{18} (mJy) (10)	S/N (11)	F (12)	V_h / V_0 (km s^{-1}) (13)	W_{50} (km s^{-1}) (14)	FI / FI_c (Jy km s^{-1}) (15)	S_{21} (mJy) (16)	q (17)	log L_{FIR} (W) (18)	log L_{21} (W Hz^{-1}) (19)	log L_B (W) / M_B (mag) (20)	log M_H ($M_\odot$) (21)
3.8	10	1	2178	160	5.34	(161)	2.43	37.03	24.89	36.69	9.09
3.6			2343		9.45					−19.91	
...	...	...	(856)	...	54.6[a]	384	2.37	36.65	21.71	36.24	9.7[a]
3.7			...		187.[a]					−18.8	
3.2	...	2	(8222)	...	1.04[b]	(78)	2.30	37.70	22.83	...	9.28[b]
...			...		1.14[b]					...	
1.8	25	1	1564	233	9.34	(72)	2.20	36.19	21.41	35.93	8.94
3.0			1726		12.34					−18.0	
4.4	6	2	9748	138	5.67	74	2.19	37.71	22.95	37.40	10.13
...			9967		5.73					−21.7	
1.6	17	2	4553	412	7.22	5	2.27	36.98	22.14	36.62	9.64
1.4			4738		8.22					−19.7	
1.9	3	2	4936	299	4.20	(61)	2.21	37.08	22.29	36.61	9.44
1.4			5158		4.41					−19.7	
1.7	...	1	(3448)	...	...	(58)	2.10	35.93	21.25	35.49	...
2.4			...		...					−16.9	
3.1	28	2	3912	403	28.44	97	2.35	37.22	22.29	37.02	10.11
1.5			4088		32.99					−20.73	
1.6	29	2	4142	281	11.89	79	2.26	37.09	22.25	36.77	9.73
0.9			4329		12.24					−20.1	
0.9	86	1	3641	403	26.67	83	2.22	36.95	22.16	36.76	10.03
0.8			3787		31.73					−20.1	
1.8	11	2	7011	251	3.95	(42)	1.41	36.40	22.41	36.44	9.68
1.3			7132		...					−19.3	
3.5	4	2	7508	107	1.14	48L	1.40L	36.50	22.53L	36.60	9.20
1.4			7640		...					−19.7	
...	...	...	(6540)	...	...	44L	1.32L	36.27	22.37L	36.39	...
1.7			...		...					−19.2	
2.1	36	2	3482	182	11.54	41	2.10	36.47	21.80	36.30	9.55
1.7			3554		12.00					−18.9	
1.8	19	2	5296	351	10.53	79	2.20	37.21	22.44	36.17	9.87
1.1			5354		10.85					−18.6	
1.4	...	2	(9990)	...	...	12L	1.91L	36.65	22.17L	...	...
...			...		...					...	
1.1	14	1	1592	121	2.14	30	2.28	35.85	21.00	35.36	8.16
1.9			1658		2.30					−16.6	
2.2	10	2	3351	79	1.64	120	1.12	35.91	22.22	36.01	8.68
2.4			3392		1.77					−18.2	
1.7	7	2	7500	142	3.04	12L	2.50L	37.08	21.92L	...	9.61
1.1			7572		...					...	
2.8	11	2	3218	185	4.65	20L	2.13L	36.15	21.45L	36.02	9.10
4.9			3258		4.98					−18.2	
2.6	10	2	4927	74	3.42	29L	2.17L	36.68	21.94L	36.34	9.30
7.6			4963		3.46					−19.0	
2.4	16	2	4214	181	6.67	12L	2.07L	36.06	21.42L	36.29	9.48
3.7			4250		7.07					−18.9	
1.1	38	1	1971	125	6.91	103	...	...	...	...	8.82
...			1973		7.19					...	
1.5	17	1	1953	167	4.83	...	...	...	...	...	8.64
...			1955		...					...	
1.5	26	1	1964	140	6.49	110	2.15	36.43	21.71	36.14	8.81
1.1			1966		7.07					−18.5	
1.5	10	1	1904	170	2.48	...	...	...	...	...	8.33
...			1906		...					...	
1.4	18	1	1994	143	4.27	...	...	...	...	...	8.60
...			1996		...					...	
1.8	36	1	1957	345	15.39	85	2.24	36.41	21.60	36.57	9.24
1.1			1967		19.08					−19.57	
3.0	5	2	3789	283	2.93	61	2.35	36.94	22.01	36.79	9.02
2.4			3745		3.17					−20.2	
3.7	7	2	3884	62	2.43	...	...	...	...	...	8.93
...			3840		...					...	
...	...	...	(4756)	...	8.2[c]	125	1.87	36.99	22.54	36.78	9.7[c]
0.8			...		8.4[c]					−20.14	
...	...	...	(2371)	...	20.[d]	94	2.18	36.59	21.83	36.59	9.5[d]
1.1			...		24.[d]					−19.66	
2.0	5	2	(9090)	...	...	55L	1.63L	36.94	22.74L	...	...
...			...		...					...	
2.8	...	2	(6750)	...	...	40	1.66	36.59	22.35	36.43	...
0.8			...		...					−19.2	
1.6	6	2	8908	230	1.78	(11)	2.00	36.60	22.03	36.62	9.74
1.6			8992		...					−19.7	
3.0	8	2	7798	150	3.64	39	2.13	37.18	22.48	37.02	9.77
1.0			7973		3.97					−20.7	
...	...	...	(4800)	...	...	41	2.36	37.03	22.09	36.77	...
1.4			...		...					−20.1	
2.5	27	2	5443	318	21.11	(338)	2.58	38.24	23.09	36.57	...
2.0			5482	...						−19.6	
2.0	10	2	7287	173	4.18	396	1.86	37.84	23.41	36.80	...
1.4			7296	...						−20.2	

The measured continuum flux density at 1415 MHz in mJy (S_{21}) is presented in column (16). The uncertainty on this quantity is typically of order 10 mJy. If no clear detections could be extracted from the continuum observations, an upper limit was entered equal to 3 times the rms fluctuations of the scan (indicated by an *L*). Entries enclosed in parentheses indicate that no continuum observations were made on that source and the value quoted is an estimate from the level of the baseline removed from the spectra. These estimates are within 10% of the actual values as demonstrated by a comparison of baselines with drift scans for those sources for which continuum observations were made.

Column (17) shows the dimensionless quantity q defined by Helou, Soifer, and Rowan-Robinson (1985) as

$$q = \log\left(\frac{\mathrm{FIR}/3.75 \times 10^{12}\ \mathrm{Hz}}{S_{21}}\right),$$

where FIR is taken from column (9), S_{21} is the continuum flux density from column (16), and 3.75×10^{12} Hz is the frequency at 80 μm. Where only upper limits on S_{21} exist the corresponding lower limit on q has been calculated (indicated by an *L* after the value).

Distances used in calculating the quantities in columns (18)–(21) used $H_0 = h \times 100$ km s^{-1} Mpc^{-1} and the corrected velocity from column (13), line (2). For nondetected galaxies, a distance was calculated using the redshifts from Lonsdale *et al.* The log ($h^2 L_{\mathrm{FIR}}$), the FIR luminosity in watts, is listed in column (18). Column (19) lists log ($h^2 L_{21}$), the 21 cm continuum luminosity in W Hz^{-1}. Column (20), line (1) shows the log ($h^2 L_{\mathrm{B}}$), the optical luminosity in watts using the apparent magnitude from column (6), line (2) and the formula from § IV.1 of Haynes and Giovanelli (1984). Line (2) of column (20) shows the same quantity expressed in magnitudes.

Finally, column (21) lists the logarithm of the H I mass of the galaxy using the formula

$$h^2 M_{\mathrm{H}} = 2.36 \times 10^5 (hD)^2 F I_C M_\odot ,$$

where D is the distance in Mpc using the corrected velocity from column (13), line (2), and FI_C is the flux integral from column (15), line (2) or line (1) where no correction was applied.

Bicay and Giovanelli (1986) investigated the errors associated with measurements made from H I profiles of galaxies as a function of signal-to-noise ratio. From their results, we adopt the following power law as an estimate of the errors in these quantities:

$$\log(E) = a - b \log(S/N) ,$$

where E is the error in km s^{-1} for velocity measurements and fractional error for the line integral, a and b are 2.9 and 2.0 for systematic velocity measurements, 3.0 and 1.7 for width measurements and 2.0 and 1.0 for flux integral measurement, and S/N is from column (11). Typical errors calculated in this manner are less than 15 km s^{-1} for velocity measurements and less than 10% for the flux integral. The measured quantities combined with these errors are consistent with the previous observations cited below in the notes on individual galaxies.

The H I spectra for those galaxies detected at 21 cm are presented in Figures 1*a–d*. These have been Hanning smoothed to a spectral resolution of roughly twice the channel separation. The baseline which was removed prior to measurement is also plotted. The bar in each square (usually the upper right-hand corner) indicates the flux scale. Interference spikes, usually at ~1400 MHz (~4350 km s^{-1}), ~1394 MHz (~5500 km s^{-1}), and ~1385 MHz (~7500 km s^{-1}) occur in several profiles. The OH spectra for the two galaxies detected at 18 cm are shown in Figure 1*e*.

Notes on individual galaxies follow.

UGC 966.—Other 21 cm radio observations include Lewis and Davies (1973), Dickel and Rood (1978), Shostak (1978), Thonnard *et al.* (1978), Mirabel (1982), Peterson and Shostak (1974), Bottinelli, Gouguenheim, and Paturel (1981*a*), Dickey (1982), and Baan *et al.* (1985). In addition, 18 cm observations were reported by Baan *et al.* (1985). We did not detect it at 18 cm after 10 minutes total on-source observing time. The H I spectrum shows an absorption feature near 2340 km s^{-1} with a width of about 100 km s^{-1}.

UGC 1201.—Other H I line observations include Bottinelli, Gouguenheim, and Paturel (1980), Briggs *et al.* (1980), Rots (1980), Mirabel (1982), Giovanardi and Krumm (1983). The flux integral quoted in column (15) of Table 1 is taken from Giovanardi and Krumm.

III Zw 035.—This source was not detected after 5 minutes total on-source observation time. It was detected by Gordon and Gottesman (1981). The flux integral quoted in column (15) of Table 1 is from Gordon and Gottesman.

UGC 1351.—Observed by Bottinelli, Gouguenheim, and Paturel (1980).

UGC 1451.—This galaxy is 9′ from UGC 1462.

UGC 1720.—The UGC indicates a companion 2.′5 away at position angle 260°.

UGC 1768.—The interference spike at $V = 4343$ km s^{-1} did not affect the measurements. Previous observations include Dickel and Rood (1978), Peterson (1979), and Bottinelli, Gouguenheim, and Paturel (1981*b*). UGC 1767 is 2.′1 away.

UGC 2103.—Observed by Mirabel (1982). Z0234.7+2056 is 2.′6 from this galaxy at position angle 14°.

UGC 2365.—The UGC notes that U2362 is 7.′1 from U2365 and U2368 is 10.′3 away.

UGC 2970.—Observed by Thonnard *et al.* (1978).

UGC 2982.—An interference spike at $V = 5495$ km s^{-1} occurs at the edge of the profile; consequently the uncertainties on the measured quantities are somewhat larger than for other galaxies. Observed by Haynes and Giovanelli (1984).

IRAS 04144+1020.—The feature near the center of the profile is an interference spike.

IRAS 04147+0218.—This source is associated with UGC 3004/3005. The spectrum clearly shows two galaxy profiles. The *IRAS* position falls on UGC 3004 on the POSS and seems to exclude UGC 3005. We have adopted this identification for 04147+0218. Lonsdale *et al.* indicate UGC 3004 is at $z = 0.0108$ and UGC 3005 is at $z = 0.0121$. We therefore adopt the low redshift profile as our candidate identification. Due to the similarity of the two profiles as well as the two galaxies, the final identification does not significantly affect our analysis. UGC 3006 is 4′ from U3004.

UGC 3014.—An interference spike is located at $V = 4346$ km s^{-1}. Uncertainties on measured quantities are somewhat larger than for other galaxies. Observed by Bicay and Giovanelli (1986).

UGC 9903/4.—Other observations include Haynes (1981), Bottinelli, Gougenheim, and Paturel (1981*a*), and Shostak (1978).

UGC 9913.—Also known as Arp 220 = IC 4553, this interesting object has been studied in some detail by other authors. See, for example, Mirabel (1982), Baan and Haschick (1984), and Rieke *et al.* (1985) for H I and OH results and Young *et al.*

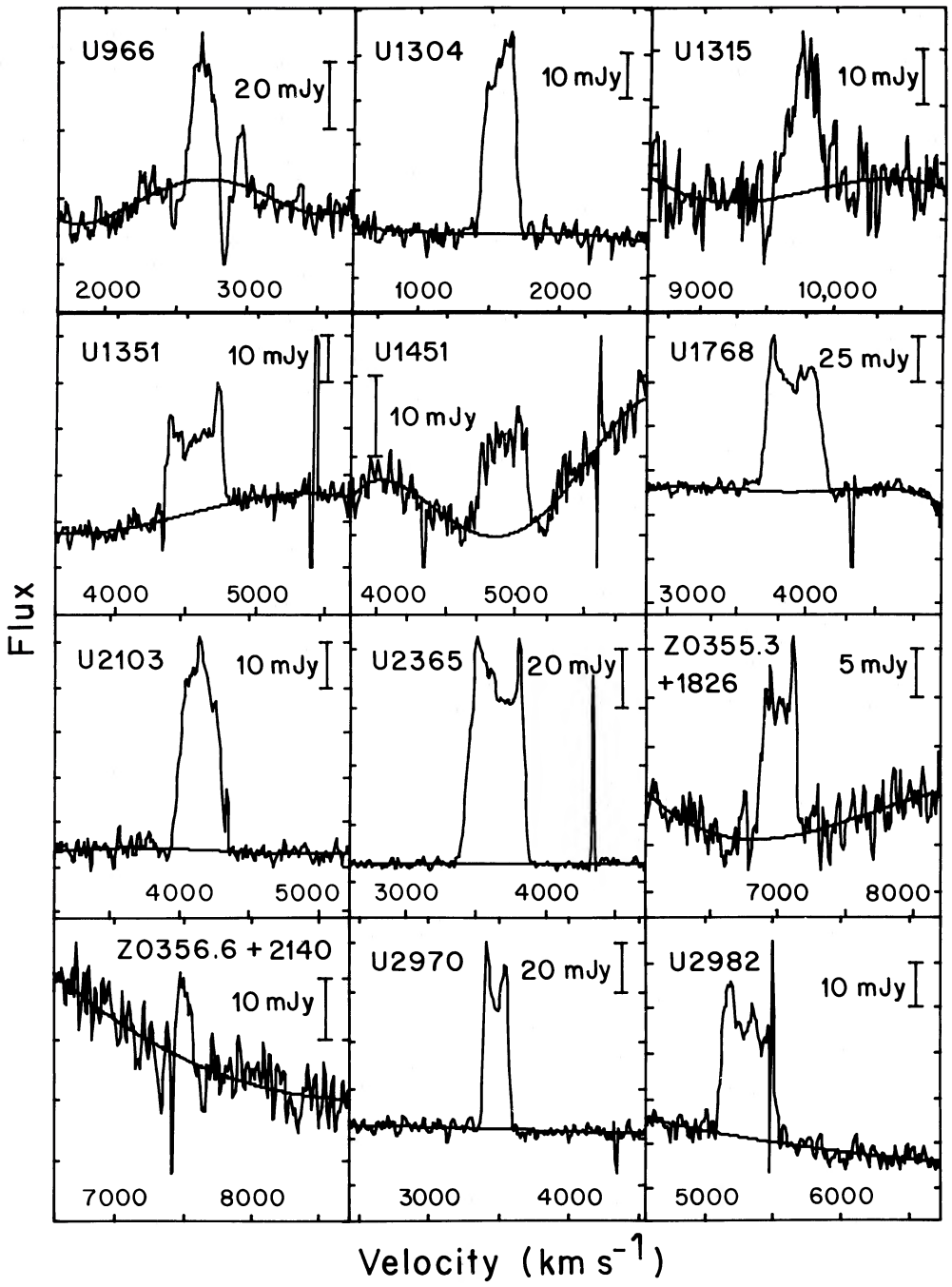

FIG. 1*a*

FIG. 1.—(*a*)–(*b*) The spectra observed from Arecibo at λ21 cm. The baselines subtracted in reduction are shown superposed on the smoothed data. Interference spikes have not been removed. The abscissa is labeled in heliocentric velocity.

(1984) and Sanders and Mirabel (1985) for CO results. There is an interference spike located at $V_h = 5672$ km s^{-1} near the edge of the H I profile. The OH profile is shown in Figure 1*e*.

UGC 9926.—Previous observations include Bottinelli *et al.* (1970), Bottinelli and Gouguenheim (1976), Shostak (1978), Krumm and Salpeter (1980), Bottinelli, Gouguenheim, and Paturel (1981*a*).

UGC 10024.—The UGC notes two galaxies nearby, Z1543.7+0236 (this is the companion position observed) and Z1543.2+0234.

UGC 10182.—Other 21 cm observations include Biermann, Clark, and Fricke (1979), Casini, Heidmann, and Tarenhi (1979), Beiging and Biermann (1983), Gordon and Gottesman (1981), Giovanelli, Chincarini, and Haynes (1981). The flux integral quoted in column (15) of Table 1 is from Beiging and Biermann.

UGC 10439.—Other 21 cm observations include Bottinelli and Gouguenheim (1976), Shostak (1978), Krumm and Salpeter (1980), and Bottinelli, Gouguenheim, and Paturel (1981*b*). The flux integral quoted in column (15) of Table 1 is from

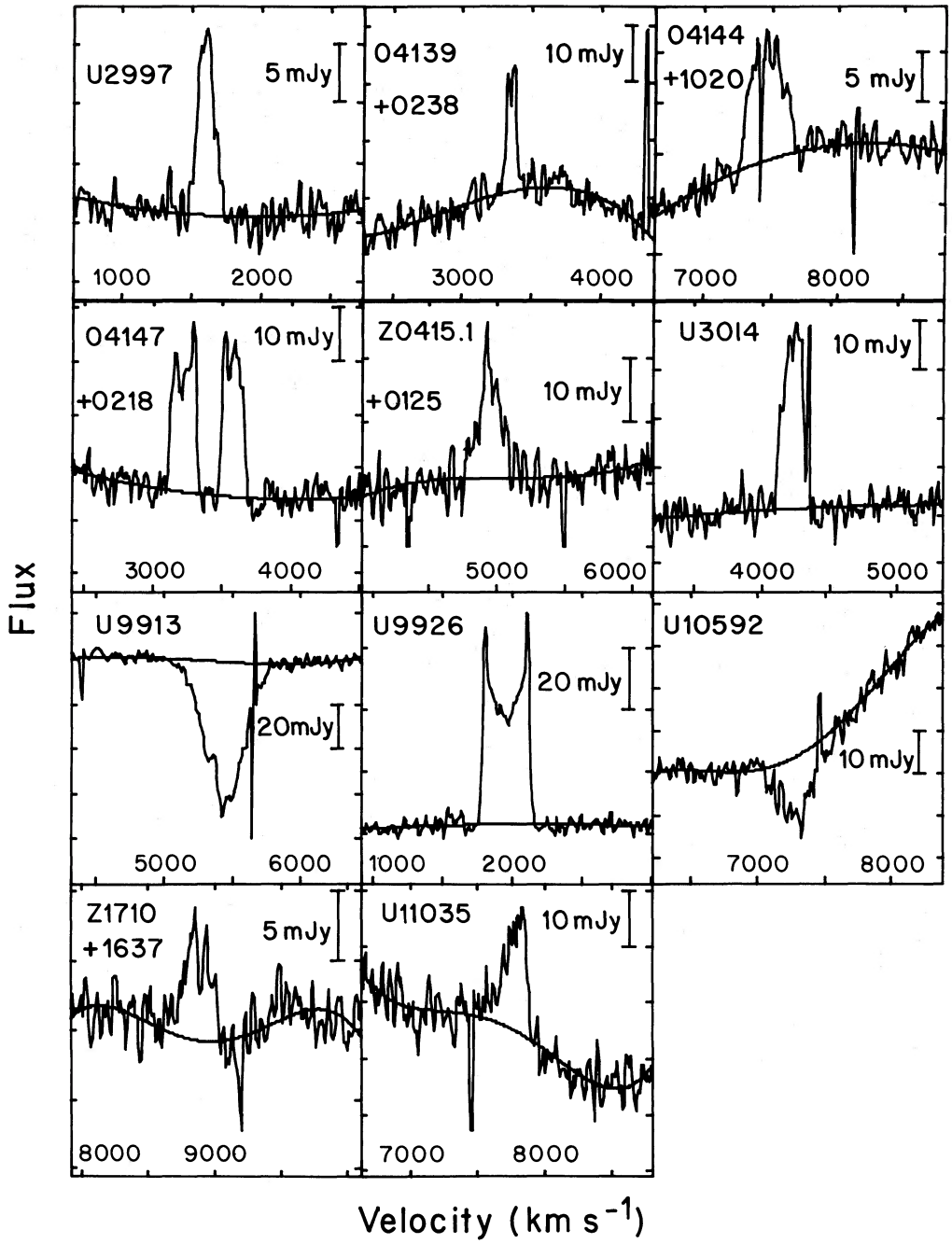

FIG. 1*b*

Krumm and Salpeter. The UGC notes a companion 3'.9 away at position angle 108°.

UGC 10592.—Also known as NGC 6240, this object, like Arp 220, has been studied in great detail by other authors (see Heckman *et al.* 1983; Wright, Joseph, and Meikle 1984; Baan *et al.* 1985; Rieke *et al.* 1985 for H I and OH results, and Young *et al.* 1986, and Sanders and Mirabel 1985 for CO results). The feature near 7500 km s^{-1} in the H I profile is an interference spike.

IV. ANALYSIS AND INTERPRETATION

a) Neutral Hydrogen Profiles

One of our objectives was to discover new cases of H I absorption and OH maser emission in these galaxies. This FIR-selected sample contains several previously known cases of H I absorption but no new absorption lines were detected. This null result is important both because it gives us some statistics of the occurrence of these phenomena in FIR-intense

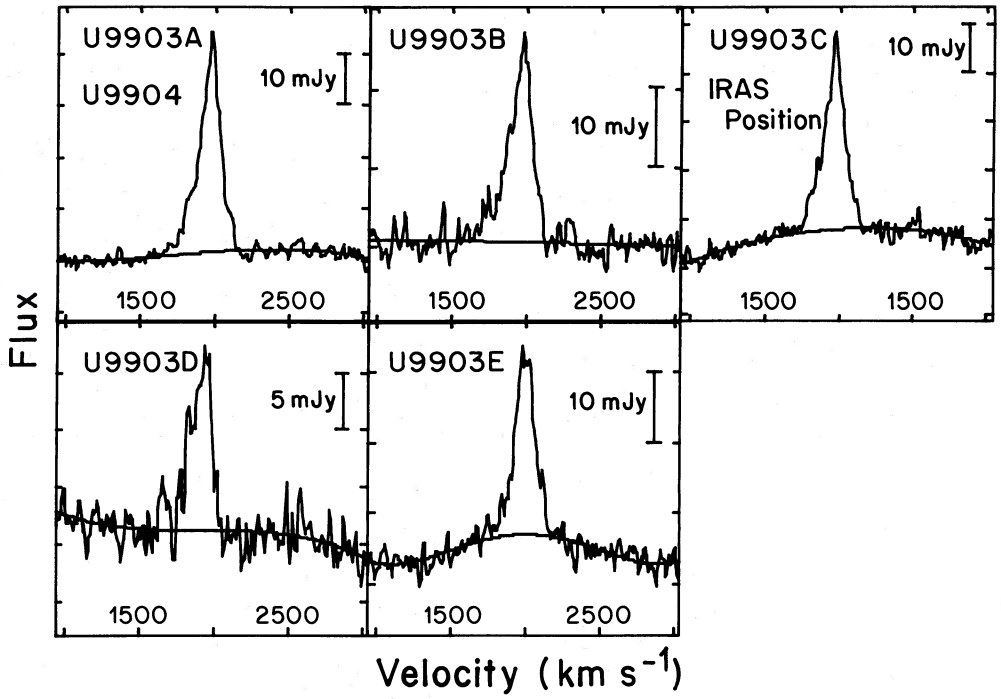

FIG. 1c

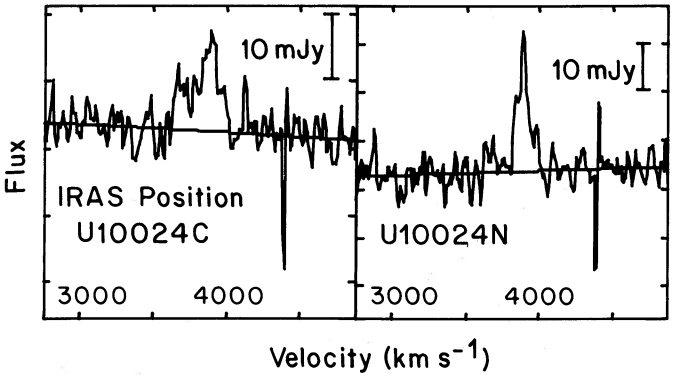

FIG. 1d

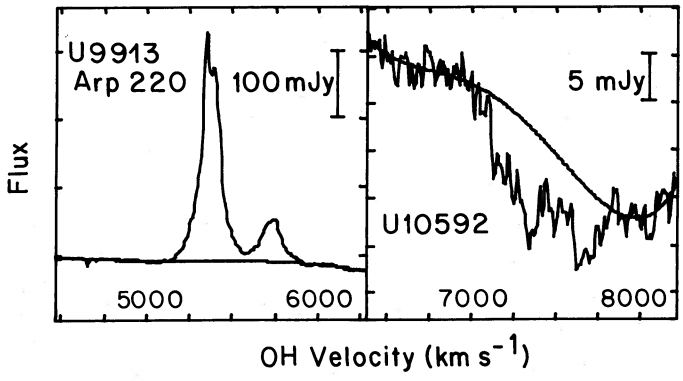

FIG. 1e

FIG. 1.—(*c*) H I spectra from five positions around U9903. (*d*) H I spectra from U10024 and its companion. (*e*) OH spectra of two galaxies with prominent OH lines.

galaxies, and because it affects the interpretation of the absorption lines in the previously known cases.

The large beam of a single dish telescope like Arecibo blends together the H I emission and absorption from a galaxy. In order for the absorption to dominate the emission requires not only that there be an intense continuum source present, but that around (or at least in front of) this source there must be a concentration of gas. The requirement for absorption to be visible is

$$\frac{M}{N} \lesssim 10^3 \frac{S_c d^2}{T} \frac{\Delta V_{\rm em}}{\Delta V_{\rm abs}}, \qquad (1)$$

where M is the total mass of H I seen in emission (in solar masses), N is the column density of H I in front of the continuum source (in units of 10^{18} cm^{-2}), S_c is the continuum flux density in Jy, d the distance in Mpc, T the mean spin temperature of the gas in units of 100 K, and $\Delta V_{\rm em}$ and $\Delta V_{\rm abs}$ the velocity widths of the emission and absorption lines. A typical path through the Milky Way disk in the solar neighborhood would have $N \approx 200$ in these units ($T = 100$ K), whereas M for the Milky Way is 2 to 3 $\times$ 10^9, thus observing our Galaxy from 10 Mpc would require a 100 Jy source behind a typical disk region to show absorption. To get a rough idea of what this restriction means for the geometry of the gas in the Galaxy we consider the idealized case of a homogeneous disk of gas of radius R (kpc) with the continuum source at the center, seen at inclination angle θ. The requirement of equation (1) becomes

$$R^2 < 0.06 \frac{S_c d^2}{T} \frac{\Delta V_{\rm em}}{\Delta V_{\rm abs}} \sec \theta . \qquad (2)$$

This assumes that the continuum source has about the same size as the disk thickness. A calculation of the effect of different nuclear source sizes has been made by Heckman *et al.* (1983).

The FIR flux from spiral galaxies correlates well with radio continuum flux, as discussed below, so a FIR-selected sample will naturally be rich in galaxies with high centimeter-wave luminosities ($S_c \times d^2$ in eqs. [1] and [2]). The galaxy with the

highest luminosity in our sample is U1201 = NGC 660 which was observed at 21 cm by Mirabel (1982) and Bottinelli, Gouguenheim, and Paturel (1980). It shows neither an OH maser nor H I absorption, which is evidence that there is no concentration of gas near the nucleus; it must have instead a hole in its H I surface density near the continuum source. U10592 = NGC 6240 has the next highest luminosity in our sample, and U9913 = IC 4553 is third. Both of these galaxies show H I absorption which overwhelms the emission at all velocities ($\Delta V_{\rm abs} \gtrsim \Delta V_{\rm em}$); in IC 4553 the line is particularly deep and broad, probably because the absorbing gas is concentrated near the nucleus as indicated by details of the OH and H_2CO emission. (Baan and Haschick 1984; Baan, Gusten, and Haschick 1986).

The single-disk model in equation (2) may not be realistic, since the absorption could be due to a small gas concentration near the nucleus quite separate from the much larger galaxy disk (Dickey 1986), especially since the amount of gas required for the absorption is miniscule compared to the total seen in the disk emission. The H I mass needed to give $N = 10^{21}$ cm^{-2} is only 10^5 $M_\odot$ in front of a typical continuum source with a 100 pc diameter and is less for smaller source diameters. It is the presence or absence of such a cloud in front of the nucleus, rather than the luminosity of the nuclear source, which may determine whether or not a galaxy like NGC 520 will show absorption. NGC 520 (=UGC 966) shows an absorption line with $\Delta V_{\rm abs} \ll \Delta V_{\rm em}$, even though its value of Sd^2 is lower than the sample median.

Although both our sample and the number of detected H I absorption lines are small, we can draw some rough conclusions about the probability of finding H I absorption in larger surveys of galaxies selected for their FIR or radio continuum flux. For a single dish it is always better to choose the most distant objects from such a sample, since it is the luminosity rather than the flux which appears in equation (1). Out of four galaxies with $Sd^2 > 50$ Jy Mpc^2 two show strong absorption. Out of 22 galaxies with $30 > Sd^2 > 1$ only one shows absorption. We need more surveys of galaxies in this lower continuum luminosity range perhaps backed up by high-resolution interferometer studies to get a better idea of the statistics of absorbing clouds near or around the nuclei of active galaxies.

Although our sample contains no new examples of nuclear clouds seen in H I absorption, this sample of galaxies does show somewhat peculiar H I emission properties. The spectra on Figure 1 show an excess of "convex" emission profiles, i.e., emission spectra which instead of showing maxima at the velocity extremes ("two-horned profiles") show rather a single peak at the velocity center. This is a relatively rare phenomenon in a volume-limited sample. A cursory analysis of 200 profiles from Giovanelli and Haynes's (1985) survey of the Perseus-Pisces supercluster shows that about 70% of galaxies have concave ("two-horned") profiles versus about 20% convex profiles. In our sample 10 out of 21 are convex, while only six out of 21 are clearly concave. Our ratio of convex to concave is thus 1.7 ± 0.5 using $(n)^{1/2}$ to estimate uncertainties, whereas a volume-limited sample would give 0.31 ± 0.05 for this ratio. Thus a FIR-limited sample has a much higher fraction of central peaked H I emission profiles than an ordinary volume-limited sample of galaxies.

This behavior in H I profiles often reflects dynamical disruption of the galaxies. Gallagher, Knapp, and Faber (1981) find that single-peaked profiles with sloping edges, like those of UGC 1315 or Z0415.1+0125, are a signature of strongly interacting galaxies. Even a sample of galaxies in small groups (not specifically selected for interaction) shows a ratio of convex to concave profile counts of 1.0 ± 0.3 (e.g. Schneider *et al.* 1986), intermediate between our sample and that of Giovanelli and Haynes (1985). This is not surprising, since many of the present galaxies show companions (see notes to Table 1). The implication is that substantial disruption of the disk often accompanies unusual infrared activity in a galaxy.

An alternative interpretation for the abundance of single-peaked profiles in this sample is that we have a higher fraction of low-mass spirals than an optically selected sample such as one based on the UGC or Zwicky catalogs. In such intrinsically faint galaxies it is not uncommon for the rotation curve to rise all the way to the outer edge of the H I disk. For such a rotation curve there is no velocity crowding of H I near the extreme rotation velocities, so two peaks are not seen in the emission spectrum. An extreme case of this is an H I disk in solid-body rotation throughout, whose single-dish profile is a half circle. Since this sample is selected by FIR rather than optical flux there are many optically faint galaxies included, and the median M_B is $-19.6+5 \log h$. Convex profiles are more common among the lower luminosity galaxies, where the shape may not imply disruption or interaction. In this case the abundance of this shape profile in this sample is still a result of different selection criterion, but not causally related to the FIR emission mechanism. This question highlights the limitations inherent in statistical comparisons when the samples are selected in different ways.

b) *Comparison of Infrared and Radio Continuum*

In Figure 2, FIR luminosity (*lower panel*) and radio continuum luminosity (*upper panel*) are plotted against optical luminosity. The best log-log fit is shown in each panel. Little correlation is evident here. It is clear however that the typical infrared-to-blue ratio is greater than one, and several times greater than the ratio for normal spirals in optically selected samples (Helou 1986*a*; de Jong *et al.* 1984). Even after correction for internal and Galactic extinction, this sample remains high in infrared-to-blue ratio, as well as in 60 to 100 micron ratio, as expected for an infrared-selected sample.

Figure 3 shows the relationship between FIR luminosity and the 21 cm radio continuum luminosity. There is a fairly good correlation between these two, although a few galaxies are discrepant. The best-fit line to the data has a regression coefficient of $R = 0.85$. If the two galaxies with the lowest values of q (*IRAS* 04139+0238, Z355.3+1826) are omitted from the fit, the value of R increases to 0.94. This radio-infrared correlation has now been established for a variety of samples of spiral galaxies (see in particular Helou, Soifer, and Rowan-Robinson 1985, but also Dickey and Salpeter 1984; Sanders and Mirabel 1985; Gavazzi, Cocito, and Vettolani 1986; Condon and Broderick 1986; and Hummel 1986). Among galaxies detected here, q has a mean value of 2.16 with a dispersion of 0.4, consistent with the values reported by Helou, Soifer, and Rowan-Robinson (1985) and Condon and Broderick (1986). An examination of the Palomar Observatory Sky Survey plates near *IRAS* 04139+0238 and Z355.3+1826 seems to exclude the possibility that their radio continuum fluxes have been contaminated by nearby bright sources. The confusion level (1 σ) for Arecibo at 1.4 GHz is about 2 mJy. Thus except for U1351 our flux values are little affected by this problem, since the noise level on our drift scans is typically greater than or $\sim$4 mJy.

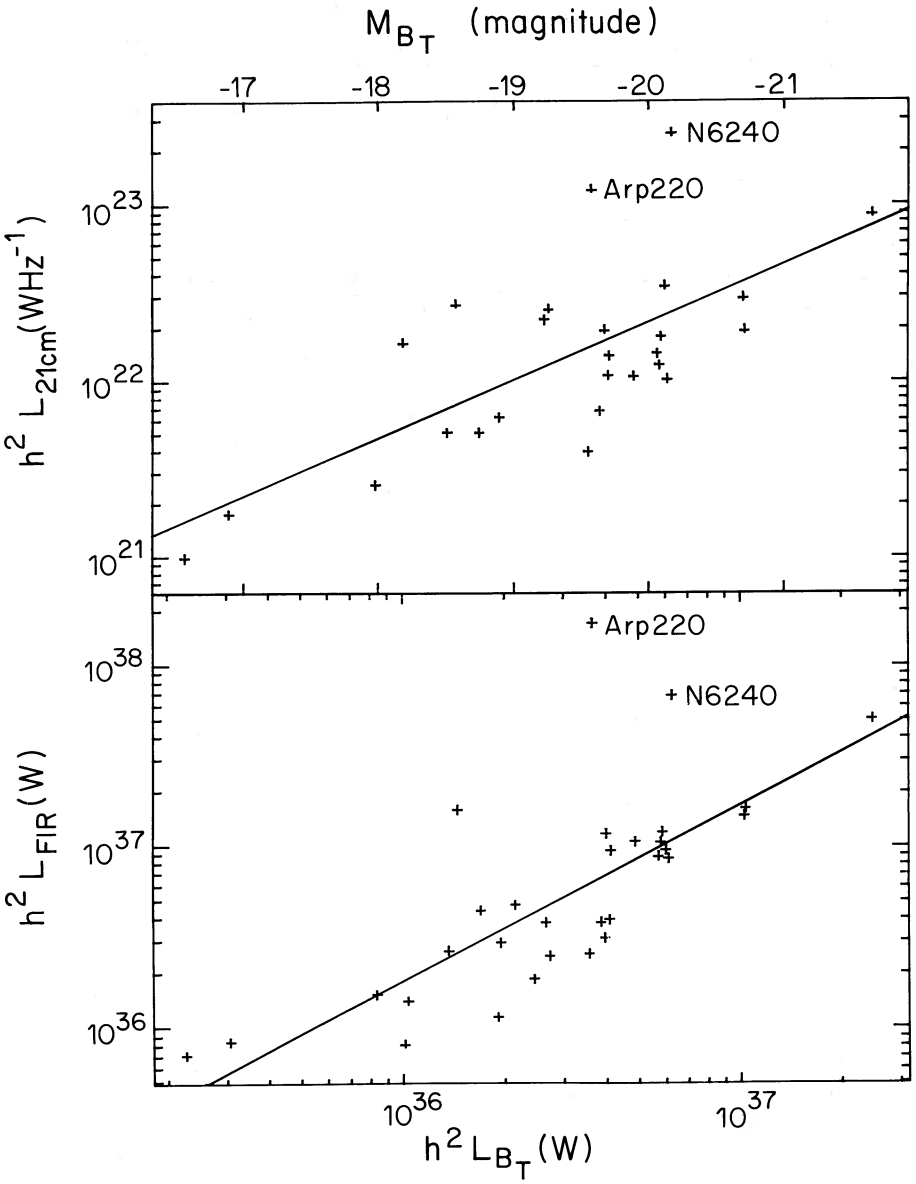

FIG. 2.—The relationships between blue luminosity (lower abscissa scale labeled in watts, upper scale in *B* absolute magnitudes) and radio continuum and FIR luminosities for galaxies in this sample.

The significance of confirming here the radio-infrared correlation is that the present sample is infrared-selected, and therefore biased toward more active galaxies, with much warmer 60/100 micron colors than found in typical spirals. According to the model by Helou (1986*b*), this contrast in color reflects the difference between systems whose infrared emission is dominated by warm active regions of star formation, and those whose emission comes mostly from the cool diffuse interstellar medium. (We leave out of the discussion possible contributions from active nuclei.) When the infrared-radio correlation applies to both ends of the color distribution, it acquires a qualitatively new meaning, for it seems constrained to apply to both active and diffuse components of infrared emission with the same ratio and same low dispersion. It is quite reasonable to expect that if low-mass stars can contribute to infrared emission by heating dust, the associated Type I supernovae can contribute to radio emission by accelerating cosmic rays. Satisfying that expectation however does not entail the observed constancy of q, because of the variable optical depth effects that enter into dust heating (Helou 1986*b*), and the possibly variable contribution to q by stars of different masses. Even if the latter variability is neglected, the simplest assumption still needed would be that Type I supernovae explode in quite diffuse regions which trap and extract synchrotron radiation from cosmic rays much less efficiently than the denser media with more intense magnetic fields where the massive stars go supernova. In spite of all these variable factors affecting it, q remains surprisingly constant as a galaxy moves from an active regime to a quiescent one.

At the other end of the activity range, even the most intense starburst galaxies such as NGC 6240 show still the same values of q. To the extent that radio emission starts only after the first stars have gone supernova, and as no starbursts have been observed with large values of q, it is quite unlikely that a star-

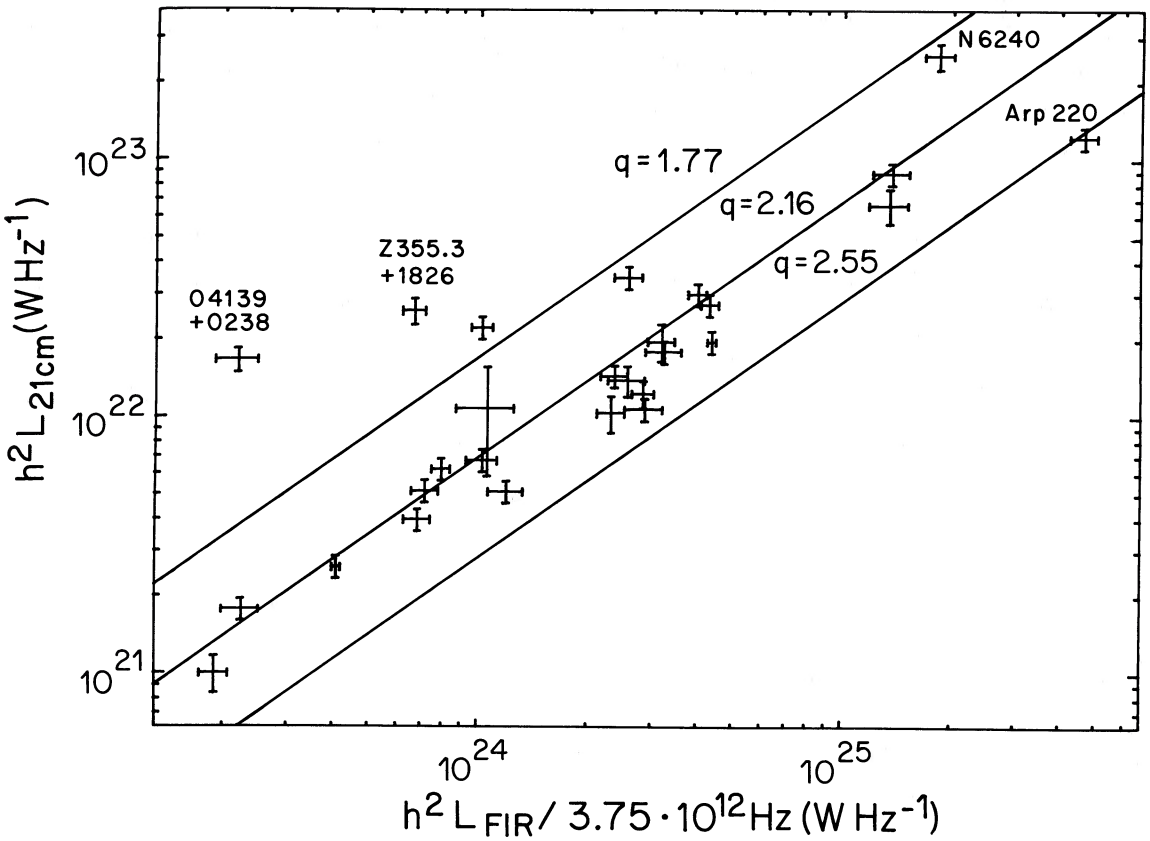

FIG. 3.—The relationship between radio continuum luminosity and FIR luminosity. Three values of q are indicated.

burst could grow to full force in less than a few times 10^7 years, the main-sequence lifetime of a 10 $M_\odot$ star.

c) *Comparison of Infrared and* H I *Emission*

Figure 4 illustrates the relation of infrared emission to H I content for the objects observed (*filled circles*). For comparison, we show from Helou (1986*a*) preliminary data on Virgo spirals (*pluses*), and a group of blue compact dwarf (BCD) galaxies (*triangles*). Also indicated are values expected from the Galactic cirrus model by Draine and Anderson (1984), and from similar calculations by Desert (1986). Following the notation of Mathis, Mezger, and Panagia (1983), χ characterizes the energy density of the interstellar radiation field heating the grains and has a value of one in the solar neighborhood. Variations in the grain-size distributions give the range of predictions indicated by the lines on Figure 4 for the same values of χ. Neglecting optical depth effects (probably a good approximation up to $\chi \approx 10$), the sequence of points from Draine and Anderson (1985) and Desert (1986) provides an approximate "heating curve" describing the emission from uniformly heated H I clouds.

The interpretation of Figure 4 is complicated by at least two factors. First, not all of the neutral hydrogen in a galaxy is participating in the infrared emission; and second, media other than the one traced by H I will contribute to that emission. Still, the heating models appear as an envelope to the right of the galaxy data. Even though the mixing of emission from active and quiescent regions within a galaxy is expected to broaden the galaxy distribution away from and to the left of the heating curve, the data in Figure 4 scatter too far to the left for that effect alone. This bias suggests a picture where a large fraction of the H I content of most galaxies is inactive at 100 microns, but where the active fraction of the H I medium provides most of the infrared emission anyway. If the latter were not true, more systems would be found to the right of the heating curve than is now the case.

As might be expected, some overlap is evident between the present sample and the Virgo spirals, but the infrared-selected sample is strongly biased toward higher $f_\nu(60\ \mu m)/f_\nu(100\ \mu m)$ ratios, and higher infrared to H I ratios. By all indications, the interstellar medium in the infrared-selected galaxies is subjected to a radiation field at least several times more intense than that seen in the solar neighborhood. Moreover, infrared-selected galaxies are found closer to the heating envelope, suggesting that a larger fraction of their neutral medium is active compared to other galaxies, or alternatively, that more of their emission comes from dust within H II regions, or possibly within molecular clouds. In Virgo galaxies, the two quantities plotted in Figure 4 seem to be uncorrelated, with galaxies scattered to high values on either axis independently of the other. The infrared-selected sample, on the other hand, seems to exhibit some correlation between the two axes. This may be due to a more concentrated distribution of H I in these active galaxies, leading to more frequent and significant H I absorption affecting the estimate made of the total H I content. This suggestion is aided by the fact that the ratio of infrared to H I in these galaxies is even higher than in BCD objects which are known to harbor intense star-formation activity, and by the

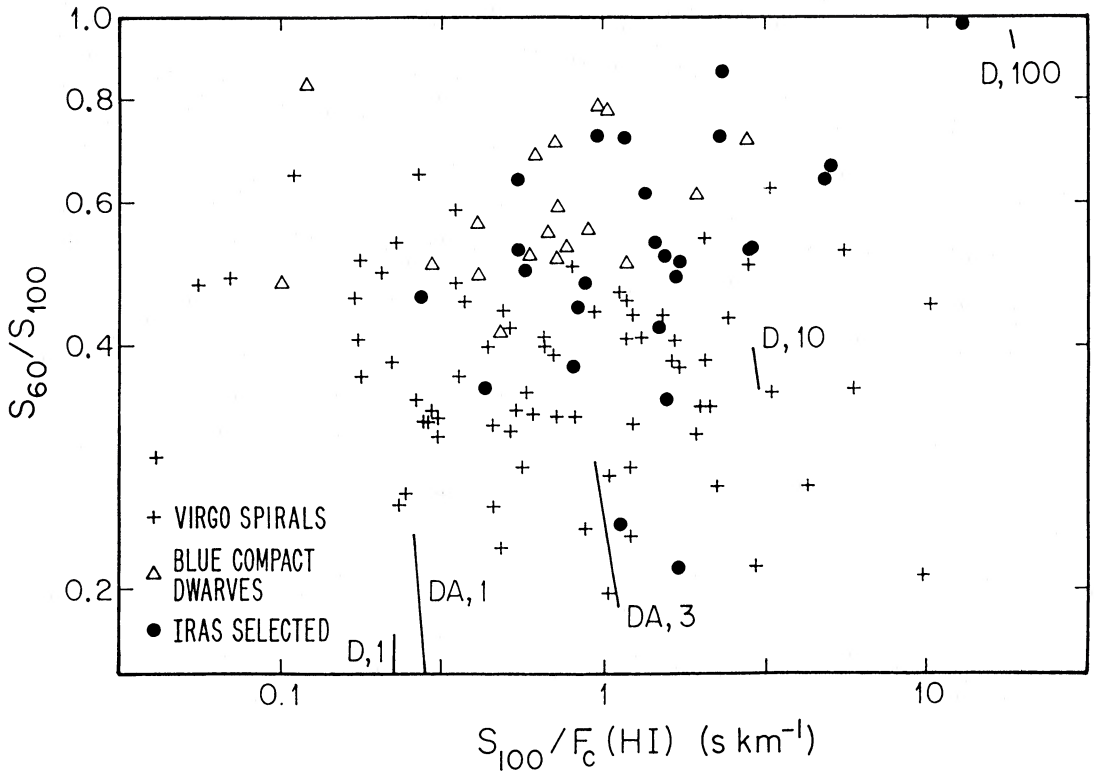

FIG. 4.—The ratio of FIR flux to 21 cm line flux plotted against FIR color. Predictions of grain emissivity models by Draine and Anderson (1985, DA) and Desert (1986, D) for values of $\chi = 1, 3, 10$, and 100 are shown.

cases of Arp 220 and NGC 6240 (detected only in absorption at the 21 cm line), and UGC 966 which shows a clear absorption feature (Fig. 1*a*).

V. CONCLUSION

The goal of this study has been to obtain a coherent set of observations of the 21 cm and 18 cm line and continuum emission from a sample of galaxies selected for their intense FIR flux. Although some had been observed previously, we have reobserved several to maintain consistent sensitivity and instrumental parameters. Four interesting results have come out of this study.

The absence of any new cases of H I absorption or OH maser emission was a surprise. The explanation (§ IV*a*) must be that concentrated nuclear starburst events embedded in an H I envelope are rare. Objects like Arp 220 are qualitatively different from galaxies with FIR luminosities a factor of 3 to 10 weaker in their OH and H I properties. In the weaker (but still abnormally FIR luminous) galaxies the starburst activity is apparently distributed over at least part of the disk, whereas in Arp 220 and NGC 6240 the continuum nucleus is surrounded by a cloud of dust and gas a few hundred parsecs or less in extent. This cloud apparently dominates the galaxy's FIR emission and its H I and OH spectra. If the FIR emission from the other galaxies in this sample were also dominated by a nuclear cloud we would expect to see more cases of H I absorption.

By comparing the FIR with the H I emission we can get a better idea of the properties of the emission regions in these galaxies. Although there is no correlation between these quantities, comparison with predictions of models of grain emissivity (§ IV*c*) show that the FIR emission per gas atom is much higher in these galaxies than in normal spirals or in the solar neighborhood. Evidently a larger fraction of the FIR emission from these galaxies is from an environment with an intense radiation field, such as an H II region.

The constancy of q, the FIR to radio continuum ratio, is the most puzzling result of this study. Although a good correlation between these two quantities had been noted before for samples of normal galaxies, the surprise is that these much more active spirals show exactly the same correlation with the same value of q. Many possible effects, such as short-duration starbursts or different mixtures of Type I and Type II supernovae, could have justified variations in q by as much as an order of magnitude; the fact that almost all these galaxies fit in the range $1.75 < q < 2.5$ (also typical for ordinary spirals) shows that none of these effects is very important.

The final result is the high fraction of galaxies in this sample which show convex (single-peaked) H I profiles compared with samples of ordinary spirals. This may suggest disruption of the circular rotation of the disk or at least a lack of H I on the flat part of the rotation curve. To understand the significance of this will require study of a larger sample, perhaps supplemented in particular cases with aperture synthesis observations.

We would like to thank Carol Lonsdale and Tom Soifer for providing data prior to publication. We are particularly grateful to the anonymous referee for constructive suggestions and criticisms. G. H. is supported as part of the *IRAS* Extended Mission by the Jet Propulsion Laboratory, California Institute of Technology, under contract with NASA. R. W. G. and J. M. D. are supported by grants from NASA JPL/957243 and NSF AST82-16879 to the University of Minnesota.

REFERENCES

Baan, W. A., Gusten, R., and Haschick, A. D. 1986, *Ap. J.*, **305**, 830.
Baan, W. A., and Haschick, A. D. 1984, *Ap. J.*, **279**, 541.
Baan, W. A., Haschick, A. D., Buckley, D., and Schmelz, J. T. 1985, *Ap. J.*, **293**, 394.
Beichman, C. A., Soifer, B. T., Helou, G., Chester, T. J., Neugebauer, G., Gillett, F. C., and Low, F. J. 1986, *Ap. J.* (*Letters*), **308**, L1.
Bicay, M. D., and Giovanelli, R. 1986, *A.J.*, **91**, 705.
Beiging, J. H., and Biermann, P. 1983, *A.J.*, **88**, 161.
Biermann, P., Clark, J. N., and Fricke, K. J. 1979, *Astr. Ap.*, **75**, 19.
Bottinelli, L., Charanaux, P., Gouguenheim, L., and Lauge, R. 1970, *Astr. Ap.*, **6**, 453.
Bottinelli, L., and Gouguenheim, L. 1976, *Astr. Ap.*, **47**, 381.
Bottinelli, L., Gouguenheim, L., and Paturel, G. 1980, *Astr. Ap.*, **88**, 32.
Bottinelli, L., Gouguenheim, L., and Paturel, G. 1981*a*, *Astr. Ap. Suppl.*, **44**, 217.
Bottinelli, L., Gouguenheim, L., and Paturel, G. 1981*b*, *Astr. Ap.*, **113**, 61.
Bridle, A. H., Davis, M. M., Fomalont, E. B., and Lequeux, J. 1972, *A.J.*, **77**, 409.
Briggs, F. H., Wolfe, A. M., Krumm, N., and Salpeter, E. E. 1980, *Ap. J.*, **238**, 510.
Casini, C., Heidmann, J., and Tarenghi, M. 1979, *Astr. Ap.*, **73**, 216.
Catalogued Galaxies and Quasars Observed in the IRAS Survey. 1985, prepared by C. J. Lonsdale, G. Helou, J. C. Good, and W. Rice (Pasadena: Jet Propulsion Laboratory).
Condon, J. J., and Broderick, J. J. 1986, *A.J.*, **92**, 94.
de Jong, T., Clegg, P. E., Soifer, B. T., Rowan-Robinson, M., Habing, H. J., Houck, J. R., Aumann, H. H., and Raimond, E. 1984, *Ap. J.* (*Letters*), **278**, L67.
Désert, F. X. 1986, in *Light on Dark Matter*, *Proc. First IRAS Conf.*, held in Noordwijk, 1985, June 10–14, ed. F. P. Israel (Dordrecht: Reidel), p. 213.
de Vaucouleurs, G., de Vaucouleurs, A., and Corwin, H. G. 1976, *Second Reference Catalogue of Bright Galaxies* (Austin: University of Texas Press), (RC2).
Dickel, J. R., and Rood, H. J. 1978, *Ap. J.*, **223**, 391.
Dickey, J. M. 1982, *Ap. J.*, **263**, 87.
Dickey, J. M. 1986, *Ap. J.*, **300**, 190.
Dickey, J. M., and Salpeter, E. E. 1984, *Ap. J.*, **289**, 461.
Draine, B. T., and Anderson, N. 1985, *Ap. J.*, **292**, 494.
Gallagher, J. S., Knapp, G. R., and Faber, S. M. 1981, *A.J.*, **86**, 1781.
Gavazzi, G., Cocito, A., and Vettolani, G. 1986, *Ap. J.* (*Letters*), **305**, L15.
Giovanardi, C., and Krumm, N. 1983, *A.J.*, **88**, 1719.
Giovanelli, R., Chincarini, G., and Haynes, M. P. 1981, *Ap. J.*, **247**, 383.
Giovanelli, R., and Haynes, M. P. 1985, *A.J.*, **90**, 12.
Gordon, D., and Gottesman, S. T. 1981, *A.J.*, **86**, 161.
Haynes, M. P. 1981, *A.J.*, **86**, 1126.
Haynes, M. P., and Giovanelli, R. 1984, *A.J.*, **89**, 758.
Heckman, T. M., Balick, B., van Breugel, W. J. M., and Miley, G. K. 1983, *A.J.*, **88**, 583.
Helou, G. 1986*a*, in *Star-Forming Dwarf Galaxies and Related Objects*, *Proc. Workshop*, held in Paris, 1985 July 1–3, ed. D. Kunth, T. X. Thuan, and J. Tran Tranh Van (Gif-sur-Yvette: Editions Frontieres).
Helou, G. 1986*b*, *Ap. J.* (*Letters*), **311**, L33.
Helou, G., Soifer, B. T., and Rowan-Robinson, M. 1985, *Ap. J.* (*Letters*), **298**, L7.
Hummel, E. 1986, *Astr. Ap.*, **160**, L4.
Infrared Astronomical Satellite (*IRAS*) *Catalogs and Atlases: The Point Source Catalog*, 1985 (Washington, DC: US Government Printing Office).
IRAS Circular, No. 6, 1983.
Kennicutt, R. C. 1983*a*, *Astr. Ap.*, **120**, 219.
———. 1983*b*, *Ap. J.*, **272**, 59.
Kirshner, R. P., Oemler, A., and Schechter, P. L. 1978, *A.J.*, **83**, 1549.
Krumm, N., and Salpeter, E. E. 1980, *A.J.*, **85**, 1312.
Lewis, B. M., and Davies, R. D. 1973, *M.N.R.A.S.*, **165**, 213.
Mathis, J. S., Mezger, P. G., and Panagia, N. 1983, *Astr. Ap.*, **128**, 212.
Mirabel, I. F. 1982, *Ap. J.*, **260**, 75.
Nilson, P. 1973, *Uppsala General Catalogue of Galaxies* (*Uppsala Astr. Obs. Ann.*, **6**) (UGC).
Peterson, S. D. 1979, *Ap. J. Suppl.*, **40**, 527.
Peterson, S. D., and Shostak, G. S. 1974, *A.J.*, **79**, 767.
Rieke, G. H., Cutri, R. M., Black, J. H., Kailey, W. F., McAlary, C. W., Lebofsky, M. J., and Elston, R. 1985, *Ap. J.*, **290**, 116.
Rodriguez Espinosa, J. M., Rudy, R. J., and Jones, B. 1987, *Ap. J.*, **312**, 555.
Rots, A. H. 1980, *Astr. Ap. Suppl.*, **41**, 189.
Sandage, A., and Tammann, G. A. 1981, *The Revised Shapley-Ames Catalog of Galaxies* (Washington, DC: Carnegie Institute of Washington.
Sanders, D. B., and Mirabel, I. F. 1985, *Ap. J.* (*Letters*), **298**, L31.
Schneider, S. E., Helou, G., Salpeter, E. E., and Terzian, Y. 1986, *A.J.*, **92**, 742.
Shostak, G. S. 1978, *Astr. Ap.*, **68**, 321.
Soifer, B. T., *et al.* 1984*a*, *Ap. J.* (*Letters*), **278**, L71.
———. 1984*b*, *Ap. J.* (*Letters*), **283**, L1.
Soifer, B. T., Sanders, D. B., Neugebauer, G., Danielson, G. E., Lonsdale, C. J., Madore, B. F., and Persson, S. E. 1986, *Ap. J.* (*Letters*), **303**, L41.
Thonnard, N., Rubin, V. C., Ford, W. K., Jr., and Roberts, M. S. 1978, *A.J.*, **83**, 1564.
Vorontsov-Velyaminov, B. A., and Arhipova, V. P. 1963–1974, *Morphological Catalog of Galaxies*, Vols. **2**–**5** (Moscow: Moscow State University) (MCG).
Vorontsov-Velyaminov, B. A., and Krasnogorskaja, A. A. 1962, *Morphological Catalog of Galaxies*, Vol. **1** (Moscow: Moscow State University) (MCG).
Wilson, A. S. 1987, in *Star Formation in Galaxies*, *Proc. Conf.*, 1986 June 16–19 in Pasadena, CA, in press.
Wright, G. S., Joseph, R. D., and Meikle, W. P. S. 1984, *Nature*, **309**, 430.
Yahil, A., Tammann, G. A., and Sandage, A. 1977, *Ap. J.*, **217**, 903.
Young, J. S., Schloerb, F. P., Kenney, J. D., and Lord, S. D. 1986, *Ap. J.*, **304**, 443.

JOHN M. DICKEY: Department of Astronomy, University of Minnesota, 116 Church St., SE., Minneapolis, MN 55455

ROBERT W. GARWOOD: University of Pittsburgh, Allen Hall, Pittsburgh, PA 15260

GEORGE HELOU: Infrared Processing and Analysis Center, California Institute of Technology, Pasadena, CA 91125